Refining ancient carbon dioxide estimates: Significance of coccolithophore cell size for alkenone-based pCO_2 records

Jorijntje Henderiks[1] and Mark Pagani[2]

Received 25 November 2006; revised 21 February 2007; accepted 20 March 2007; published 20 July 2007.

[1] Long-term alkenone-based pCO_2 records are widely applied in paleoclimate evaluations. These pCO_2 estimates are based on records of the carbon isotope fractionation that occurs during marine haptophyte photosynthesis ($\varepsilon_{p37:2}$). In addition to the concentration of aqueous CO_2 ($CO_{2(aq)}$) the magnitude of $\varepsilon_{p37:2}$ is also influenced by algal growth rates and cell geometry. To date, the influence of haptophyte cell geometry on the expression of ancient $\varepsilon_{p37:2}$ values has received little attention. This study evaluates changes in cell geometry of ancient alkenone-producing algae at Deep See Drilling Project Site 516 in the southwest Atlantic Ocean by analyzing individual coccolith dimensions, which are proportional to algal cell volume and surface area. We show that during part of the early Miocene, mean cell sizes of alkenone-producing algae were smaller relative to modern *Emiliania huxleyi*. Cell size variations coincide with significant changes in $\varepsilon_{p37:2}$, with a distinct 6‰ decrease in $\varepsilon_{p37:2}$ at ~20.3 Ma associated with a 27% increase in haptophyte cell sizes. These changes in cell size impact $\varepsilon_{p37:2}$-based interpretations of growth rate variation and $CO_{2(aq)}$ estimates for this southwest Atlantic site. After correcting for cell geometry, $CO_{2(aq)}$ estimates at Site 516 are consistent with those reported from other oligotrophic sites during this time, resulting in overall low atmospheric pCO_2 estimates (<350 ppmv) for the early Miocene.

Citation: Henderiks, J., and M. Pagani (2007), Refining ancient carbon dioxide estimates: Significance of coccolithophore cell size for alkenone-based pCO_2 records, *Paleoceanography*, *22*, PA3202, doi:10.1029/2006PA001399.

1. Introduction

[2] Accurate reconstructions of pCO_2 are essential to understand how climate sensitivity to carbon dioxide has evolved through time. In the absence of direct measurements of atmospheric gases [*Siegenthaler et al.*, 2005], ancient records of pCO_2 have been estimated by various techniques [*Freeman and Hayes*, 1992; *Pagani et al.*, 1999; *Pearson and Palmer*, 2000; *Van der Burg et al.*, 1993] (see also review by *Royer et al.* [2001]). One prominent paleo-pCO_2 approach reconstructs the concentration of $CO_{2(aq)}$ in ocean surface waters using the carbon isotopic composition of C_{37} alkenones and estimates of the carbon isotopic fractionation (ε_p) that occurred during algal photosynthesis [*Jasper and Hayes*, 1990; *Jasper et al.*, 1994; *Bidigare et al.*, 1997; *Pagani et al.*, 1999]. In the modern ocean, alkenones are produced by only a few unicellular haptophytes, including the coccolith-bearing species *Emiliania huxleyi* (*E. huxleyi)* and *Gephyrocapsa oceanica* (*G. oceanica*) [*Marlowe et al.*, 1990; *Conte et al.*, 1995; *Volkman et al.*, 1995]. Although certain noncalcifying haptophytes, such as *Isochrysis galbana (I. galbana)*, also produce alkenones, they are restricted to coastal areas and therefore not considered an important source of alkenones in the open ocean [*Marlowe et al.*, 1990].

[3] While the magnitude of ε_p derived from alkenones ($\varepsilon_{p37:2}$) is a function of $CO_{2(aq)}$, it is also influenced by algal growth rates (μ) [*Bidigare et al.*, 1997], the ratio of cellular carbon content to cell surface area [*Popp et al.*, 1998; *Burkhardt et al.*, 1999], and environmental factors such as light intensity and irradiance [*Rost et al.*, 2002; *Cassar et al.*, 2006]. To minimize the influence of growth rate on Miocene pCO_2 estimates, *Pagani et al.* [1999, 2000] restricted analysis to deep-sea sediments from oligotrophic regions. However, the influence of changing cell geometry on paleo-$\varepsilon_{p37:2}$ and pCO_2 reconstructions has yet to receive detailed consideration because of a lack of an adequate proxy.

[4] Changes in cell geometry can exert considerable influence on $\varepsilon_{p37:2}$ and pCO_2 estimates. For example, larger phytoplankton cells, with higher carbon cell quota relative to surface area, fractionate less than smaller cells under similar $CO_{2(aq)}$ [e.g., *Laws et al.*, 1995; *Popp et al.*, 1998]. The cellular carbon content of marine algae is a standard measure in field- and laboratory-based experiments and can be estimated from cell volume [e.g., *Verity et al.*, 1992; *Montagnes et al.*, 1994; *Popp et al.*, 1998]. If algal cell dimensions (e.g., cell surface area and cell volume) could be accurately reconstructed from the fossil record, this would help refine paleo-$\varepsilon_{p37:2}$ and paleo-pCO_2 reconstructions. In this study, we quantitatively reconstruct temporal changes in haptophyte cell size from coccolith dimensions in deep-sea sediments, and then evaluate the influence of coccolitho-

[1]Department of Geology and Geochemistry, Stockholm University, Stockholm, Sweden.
[2]Department of Geology and Geophysics, Yale University, New Haven, Connecticut, USA.

0883-8305/07/2006PA001399$12.00

phore cell size variability on early Miocene paleo-pCO_2 reconstructions for one site in the southwestern Atlantic Ocean (DSDP Site 516).

2. Site Description

[5] DSDP Site 516 (30°16.59′S, 35°17.10′W) is located in the South Atlantic subtropical gyre on the upper flanks of the Rio Grande Rise at 1313 m water depth. The Rio Grande Rise vertically intersects several major water masses of the South Atlantic, including Antarctic Intermediate Water (AAIW) and North Atlantic Deep Water, overlain by oligotrophic surface waters [*Johnson*, 1983]. Today, Site 516 is situated north from the Northern Subtropical Front [*Belkin and Gordon*, 1996] and other frontal zones of the South Atlantic (Figure 1).

[6] *Pagani et al.* [2000] used $\varepsilon_{p37:2}$ records from Site 516 to argue for substantial changes in algal growth rates at 20 Ma that were linked to the (deep) opening of the Drake Passage and subsequent intensification of the Antarctic Circumpolar Current (ACC) and AAIW production. However, the timing of the opening of the Drake Passage and the formation of the ACC is uncertain. Estimates range from the late Eocene [see, e.g., *Scher and Martin*, 2004] to as late as 22 ± 2 Ma [*Barker and Burrell*, 1977, 1982] (see also review by *Barker and Thomas* [2004]).

[7] During the Miocene, carbonate-rich sediments were deposited at similar water depth as today [*Barker*, 1983]. These depths are well above the lysocline and calcite compensation depths, providing well-preserved calcareous nannofossils and planktic foraminifera.

3. Fossil Record of Alkenone-Producing Haptophytes

[8] In order to assess long-term $\varepsilon_{p37:2}$ trends in relationship to changes in haptophyte cell size, cell geometry analysis should be restricted to specific coccolithophorid species that synthesized alkenones in the geological past [*Marlowe et al.*, 1990; *Volkman*, 2000]. Modern *E. huxleyi* is one of the smallest and most common calcifying haptophytes in today's oceans and is widely used as a "model" coccolithophore in experimental studies [e.g., *Westbroek et al.*, 1993; *Bidigare et al.*, 1997; *Popp et al.*, 1998; *Riebesell et al.*, 2000; *Rost et al.*, 2002]. However, this species, as well as the closely related *G. oceanica* are relatively recent evolutionary additions to haptophyte diversity with origins at 291,000 ka and ~1.7 Ma, respectively [*Thierstein et al.*, 1977; *Raffi et al.*, 2006, and references therein], which arguably limits the application of the alkenone-based paleoproxies to the Pleistocene and requires careful consideration of evolutionary patterns of modern calibration taxa (see also discussion by *Volkman* [2000]). Cenozoic ancestors of *E. huxleyi* and *G. oceanica* are clearly distinguished on the basis of combined molecular [*Fujiwara et al.*, 2001; *Sáez et al.*, 2003] and micropaleontologic data [*Marlowe et al.*, 1990; *Young*, 1990, 1998].

[9] The molecular phylogenetic clade of modern coccolith-bearing haptophytes comprises two distinct clusters (Figure 2) [*Fujiwara et al.*, 2001; *Sáez et al.*, 2003]. One phylogenetic cluster, the order Isochrysidales, contains alkenone-producing taxa, including the bloom-forming species *E. huxleyi* and *G. oceanica*, as well as the noncoccolith bearing *I. galbana* [*Marlowe et al.*, 1990; *Conte et al.*, 1995; *Volkman et al.*, 1995]. The other cluster, the order Coccolithales, contains most other coccolithophores, including *Coccolithus pelagicus* and *Calcidiscus leptoporus*, which are not known to produce alkenones [e.g., *Marlowe et al.*, 1990; *Volkman*, 2000; *Rosell-Melé et al.*, 2000].

[10] *Marlowe et al.* [1990] linked the fossil coccolith record to alkenone and alkenoate occurrences in marine sediments dating back to the Eocene (~45 Ma) and assigned likely ancient haptophyte sources. Cenozoic ancestors of *Emiliania* and *Gephyrocapsa* are found within the family Noelaerhabdaceae and genera *Reticulofenestra* and *Dictyococcites* (Figure 2) [*Marlowe et al.*, 1990; *Young*, 1990, 1998]. In view of the gradual character of intergeneric variations, *Dictyococcites* is regarded as a heavily calcified, junior synonym of *Reticulofenestra* by many authors [e.g., *Wise*, 1983; *Young*, 1990; *Beaufort*, 1992]. We follow this view in considering these closely related taxa as one group, the reticulofenestrids [cf. *Young*, 1990]. Reticulofenestrids are very common or even dominant in most Neogene deep-sea deposits, characterized by elliptical coccoliths built from calcite elements with subradial c axis orientation (R units), similar to *Emiliania* and *Gephyrocapsa* [*Young et al.*, 1992].

[11] Size variation of reticulofenestrid coccoliths has been the focus of previous studies of late Miocene to late Pliocene deep-sea records in the North Atlantic [*Beaufort*, 1992; *Kameo and Takayama*, 1999], middle Miocene to Pliocene in the Indian Ocean [*Young*, 1990], and Eocene in the South Atlantic [*Backman and Hermelin*, 1986]. These studies have shown distinct variability in coccolith size but only minor differences in basic morphologic features.

4. Material and Analytical Methods

[12] A total of 24 sediment samples were selected from Holes 516 and 516F, equivalent to sample depths of earlier published $\varepsilon_{p37:2}$ data by *Pagani et al.* [2000], and includes the time interval ~21–19 Ma which was depicted as a period of major paleoceanographic change. The age model for Site 516 is presented by *Pagani et al.* [2000] with minor modifications (see auxiliary material Table S1 and references therein).[1]

4.1. Nannofossil Assemblages

[13] Nannofossil microscope slides were prepared with the spraying technique [*McIntyre et al.*, 1967; *Bollmann et al.*, 1999]. The spraying method was preferred over standard smear slides based on a reproducibility study of morphometry and proportion estimates [*Henderiks and Törner*, 2006]. Nannofloral composition was determined by counting ~550 specimens per sample at 1250x magnification using a Leitz polarizing light microscope. The dominant coccolithophore genera were identified to species or morphotype levels (see auxiliary material Text S1 for

[1] Auxiliary material data sets are available at ftp://ftp.agu.org/apend/pa/2006pa001399. Other auxiliary material files are in the HTML.

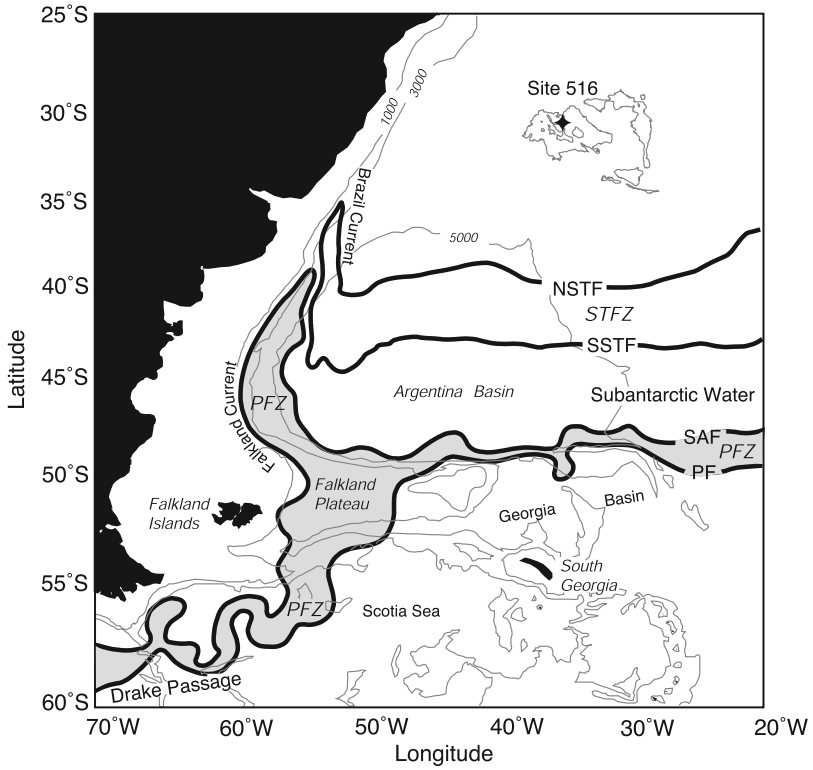

Figure 1. Location map of DSDP Site 516, Rio Grande Rise. A schematic representation of present-day upper ocean water masses and fronts is shown (modified from *Peterson and Whitworth* [1989] and *Belkin and Gordon* [1996]). Abbreviations are PFZ, Polar Frontal Zone; PF, Polar Front; SAF, Subantarctic Front; STFZ, Subtropical Frontal Zone; SSTF, Southern Subtropical Front; and NSTF, Northern Subtropical Front.

taxonomic notes). Other, subordinate nannofossil taxa were identified to genus level and will be presented elsewhere (J. Henderiks, unpublished data, 2006).

4.2. Coccolith Biometry

[14] Coccolithophores are unicellular algae that surround their cell with an armor of small calcite platelets (coccoliths), called the coccosphere. Individual coccoliths are produced inside the cell, which implies that maximum coccolith size cannot exceed the cell diameter. In the fossil record, complete coccospheres are rarely found because they collapse into separate coccoliths. In this study, a total of 55 fossil reticulofenestrid coccospheres were identified at 1250x magnification using a Leitz polarizing light microscope, and digitally recorded with a Leica DFC 320 digital camera (calibrated pixel resolution = 0.033 μm). Images taken with polarized light and a green filter enable the measurement of the outer and inner coccosphere diameter. The latter approximates cell diameter and the difference between coccosphere and cell diameter approaches the thickness of two coccoliths. In addition, multiple cross sections of coccoliths on the same coccosphere were measured. This approach constrains the relationships between individual coccolith size, coccosphere and cell diameter, which allows accurate estimates of cell dimensions based on individual coccolith size measurements in deep-sea sediments.

[15] For each sample, ~200 individual reticulofenestrid coccoliths were randomly selected from four replicate slides [*Henderiks and Törner*, 2006]. Digital images of individual coccoliths were recorded using cross-polarized light and a lambda plate to enhance color contrast. Coccolith length (or, maximum diameter) is an adequate single parameter to describe coccolith size, since it correlates strongly with other parameters such as coccolith width and central area dimensions [e.g., *Backman and Hermelin*, 1986]. All size measurements on calibrated digital images were performed using ImageJ freeware (v.1.31).

4.3. Approach to Paleo-pCO_2 Reconstruction

[16] For this study, we use previously published records of $\varepsilon_{p37:2}$ [*Pagani et al.*, 2000] calculated from the carbon isotopic compositions of alkenones ($\delta^{13}C_{37:2}$) and foraminiferal carbonate ($\delta^{13}C_{foram}$) [see *Pagani et al.*, 1999]. The magnitude of ε_p is a function of the isotope fractionations associated with carbon transport and fixation, the concentrations of extracellular and intracellular $CO_{2(aq)}$, specific growth rate, and the ratio of volume to surface area of the algal cell [e.g., *Rau et al.*, 1989, 1992; *Laws et al.*, 1995; *Bidigare et al.*, 1997; *Popp et al.*, 1998]. For field-based and

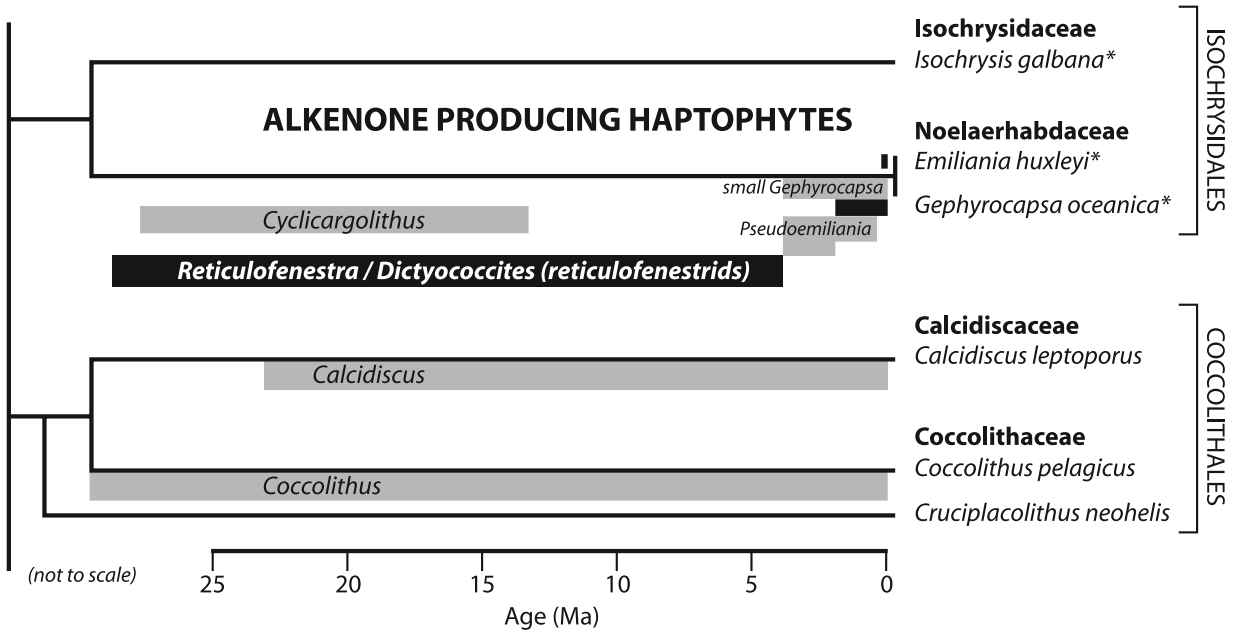

Figure 2. Simplified diagram of molecular phylogenetic relationships between extant haptophytes within the orders Isochrysidales and Coccolithales [*Fujiwara et al.*, 2001; *Sáez et al.*, 2003]. Extant haptophytes which produce alkenones (indicated with an asterisk [*Marlowe et al.*, 1990]) belong to the order Isochrysidales. On the basis of fossil coccolith morphology and crystallography the most likely Cenozoic ancestors of alkenone-producing coccolithophores *Emiliania huxleyi* and *Gephyrocapsa oceanica* are found within the family Noelaerhabdaceae, specifically the genera *Reticulofenestra* and *Dictyococcites* [*Marlowe et al.*, 1990; *Young*, 1990, 1998]. In this study, we regard *Dictyococcites* as a heavily calcified, junior synonym of *Reticulofenestra* and have grouped both as reticulofenestrids [cf. *Young*, 1990].

experimental work these factors are related to ε_p by the following expression:

$$\varepsilon_p = \varepsilon_f \frac{b}{CO_{2(aq)}} \quad (1)$$

where $CO_{2(aq)}$ is the concentration of aqueous carbon dioxide in surface water, ε_f is the carbon isotopic fractionation during carbon fixation, and the term "b" represents the sum of all physiological factors affecting carbon discrimination, such as growth rate (μ) and cell geometry.

[17] Chemostat culture experiments with different eukaryotic species (various diatoms and *E. huxleyi*) demonstrate that ε_f is ~25‰ [*Laws et al.*, 1995; *Bidigare et al.*, 1997; *Popp et al.*, 1998]. In today's ocean, the magnitude of the term "b" is related to the phosphate concentration of the surface ocean ($[PO_4^{3-}]$) [*Bidigare et al.*, 1997; *Pagani et al.*, 2005], expressed by the following relationship:

$$b = 84.07 + 118.52\left[PO_4^{3-}\right] \quad (2)$$

Modern surface water $[PO_4^{3-}]$ at Site 516 is < 0.25 μmol L^{-1} but for the Miocene a range of phosphate concentrations (0.2–0.4 μmol L^{-1}) was applied in order to capture the probable $[PO_4^{3-}]$ in the photic zone and to estimate probable values of "b". This allows calculation of $CO_{2(aq)}$, using equation (1) with measured values of $\varepsilon_{p37:2}$ and an ε_f value of 25‰.

4.3.1. How ε_p Relates to Cell Size

[18] *Popp et al.* [1998] provided evidence that the slope of the line relating ε_p to the ratio $\mu/CO_{2(aq)}$ varies by a factor greater than 20 for different species of phytoplankton and one cyanobacterium grown in chemostat culture. The slope of ε_p versus $\mu/CO_{2(aq)}$ is also linearly correlated with the ratio of carbon cell quota to surface area ratio [*Popp et al.*, 1998] which reflects the dependency of isotopic fractionation on the fluxes of CO_2 into and out of the cell. More specifically, CO_2 fluxes are proportional to cell surface area and algal growth rate, which relates to the net transport of carbon into the cell relative to its carbon biomass [e.g., *Laws et al.*, 1995]. The carbon cell quota for various algal species [*Popp et al.*, 1998] is proportional to cell volume raised to the 0.88 power, consistent with other empirical estimates [*Verity et al.*, 1992; *Montagnes et al.*, 1994]. Cell volume can therefore be considered a suitable proxy for carbon cell quota.

[19] Carbon biomass data for different coccolithophores [e.g., *Riebesell et al.*, 2000; *Zondervan et al.*, 2001; *Langer et al.*, 2006] also suggest a consistent proportional relationship with cell volume. However, because *E. huxleyi* is the only coccolithophore that has been empirically evaluated for the relationship between ε_p, $\mu/CO_{2(aq)}$, and cell geometry [e.g., *Bidigare et al.*, 1997; *Popp et al.*, 1998; *Riebesell et al.*, 2000] we assume that the influence of cell

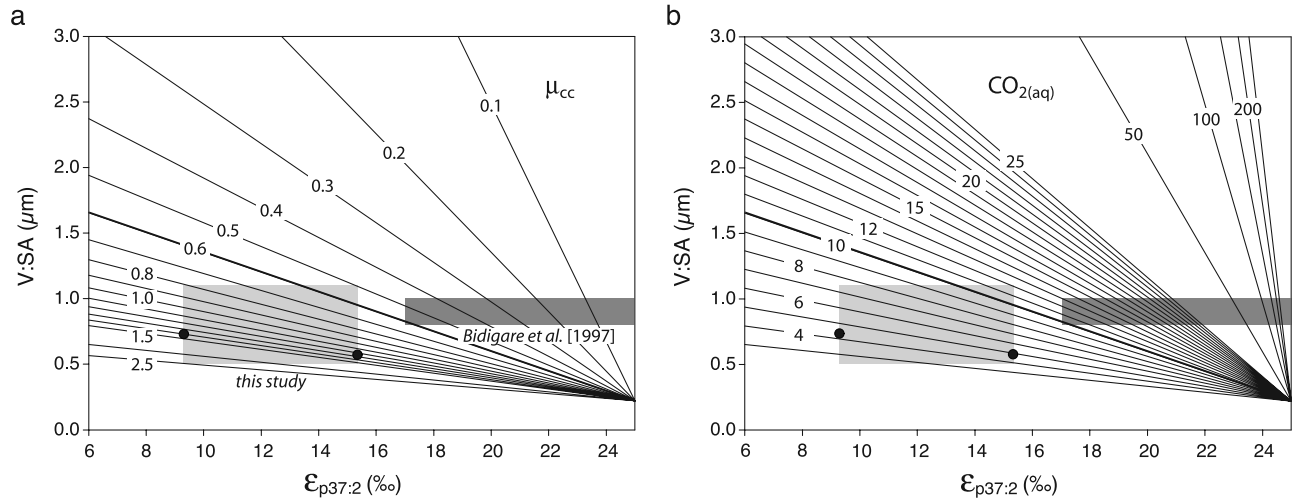

Figure 3. Relationship between $\varepsilon_{p37:2}$ (‰) and haptophyte cell V:SA (μm) using equations (4), (5a), and (5b) (following *Bidigare et al.* [1997] and *Popp et al.* [1998]), with modeled effects of (a) variable growth rate μ (day^{-1}) with constant $CO_{2(aq)} = 10$ μmol kg^{-1} and (b) variable $CO_{2(aq)}$ (in μmol kg^{-1}) with constant growth rates $\mu_{cc} = 0.6$ day^{-1}. Bold lines indicate equal conditions between plots (Figure 3a) and (Figure 3b): $\mu_{cc} = 0.6$ day^{-1} and $CO_{2(aq)} = 10$ μmol kg^{-1}. Contoured growth rates represent values under continuous-light chemostat experiments (μ_{cc}). In order to estimate natural specific haptophyte growth rates, μ_{cc} needs to be corrected for effect of day length and respiration [*Bidigare et al.*, 1997]. Under (Figure 3a) constant $CO_{2(aq)}$, and assuming diffusive uptake of CO_2, similar values of $\varepsilon_{p37:2}$ could be generated by larger algal cells (with high V:SA) with lower growth rates and/or small cells with high growth rates. On the other hand, in order to produce similar values of $\varepsilon_{p37:2}$ under (Figure 3b) constant growth rate the carbon demand of larger cells would require (and thus represent in the paleorecord) higher concentrations of $CO_{2(aq)}$ compared to smaller alkenone-producing algae. The dark grey box to the right depicts values of $\varepsilon_{p37:2}$ and V:SA as observed by *Bidigare et al.* [1997] in chemostat experiments with *E. huxleyi*. The larger lighter grey box to the left represents values observed in this study at Site 516. Circles designate the 6‰ change in $\varepsilon_{p37:2}$ at ~20 Ma with a corresponding 27% increase in mean V:SA. This implies only a minor change in haptophyte growth rates (16%), assuming no changes in $CO_{2(aq)}$.

geometry on alkenone-derived ε_p values follows the results of the multispecies study by *Popp et al.* [1998, Figure 2d] (including only eukaryotic species, $r^2 = 0.70$):

$$\varepsilon_p = 25.3 - 182\left(\frac{\mu}{CO_{2(aq)}}\frac{\text{volume}}{\text{surface area}}\right) \quad (3)$$

where the term "b" from equation (1) is now expressed by specific growth rate (μ), and the cell volume to surface area ratio (V:SA). The slope of the line defined by volume versus surface area can be defined by a constant, $K_{V:SA}$ [*Popp et al.*, 1998] (including only eukaryotic species, $r^2 = 1.00$):

$$K_{V:SA} = 49 - 222\left(\frac{\text{volume}}{\text{surface area}}\right) \quad (4)$$

4.3.2. Correcting for Haptophyte Cell Size

[20] In order to evaluate the influence of changing cell geometry on $\varepsilon_{p37:2}$ values equations (1), (3), and (4) can be recast as

$$\varepsilon_{p37:2} = \varepsilon_f - K_{V:SA}\left(\frac{\mu}{CO_{2(aq)}}\right) \quad (5a)$$

$$\left(\frac{\mu}{CO_{2(aq)}}\right) = \frac{(\varepsilon_f - \varepsilon_{p37:2})}{K_{V:SA}} \quad (5b)$$

Solutions for equation (5b) are then approached using measured $\varepsilon_{p37:2}$ values, assuming $\varepsilon_f = 25$‰, and calculating $K_{V:SA}$ from mean V:SA per sample. In this way, the covariance or variability in μ and $CO_{2(aq)}$ can be evaluated (Figure 3).

[21] Specific growth rates calculated from equation (5b) represent values under continuous-light culturing experiments (μ_{cc} [see *Bidigare et al.*, 1997]). For natural specific haptophyte growth rates μ_{cc} needs to be corrected for the effect of day length and respiration [*Bidigare et al.*, 1997]. Varying day length of 10 to 14 hours (approximate photoperiods during winter and summer solstice at 30°S) results in a correction of μ_{cc} by a factor of 0.33 to 0.47.

[22] Alternatively, the term "b" can be corrected relative to changes in V:SA, so that

$$b' = b\left[\frac{V:SA_{fossil}}{V:SA_{Ehux}}\right] \quad (6a)$$

where $V:SA_{fossil}$ is estimated from coccolith morphology in each sample, and $V:SA_{Ehux}$ is a constant value reflecting cell dimensions of the modern haptophyte *Emiliania huxleyi* in chemostat culture (cell radius = 2.6 ± 0.3 μm and $V:SA_{Ehux}$ = 0.9 ± 0.1 μm [*Popp et al.*, 1998]). Given these relationships, ancient CO_2 concentrations in seawater can then be estimated by

$$\left[CO_{2(aq)}\right] = \frac{b'}{\left(\varepsilon_f - \varepsilon_{p37:2}\right)} \quad (6b)$$

This approach is similar to that used by *Pagani et al.* [1999, 2000, 2005] in estimating past $CO_{2(aq)}$ and pCO_2 variability, but now includes both physiological factors known to influence the magnitude of $\varepsilon_{p37:2}$.

5. Results

5.1. Nannofossil Assemblages

[23] Overall changes in nannofossil assemblages include a shift in dominance from *Cyclicargolithus* (73%) during the late Oligocene to *Reticulofenestra* and *Dictyococcites* (combined, 46–80%) during the early Miocene (Figures 4c, 4d, and 4e). Remarkably, major shifts in nannofossil assemblages occur between 20.3–19.5 Ma and 18–17 Ma, coinciding with a ~6‰ decrease and a ~2‰ increase in $\varepsilon_{p37:2}$ values, respectively (Figure 4f). *Dictyococcites* (or heavily calcified reticulofenestrids [cf. *Young*, 1990]) increases in abundance by 19.5 Ma, while *Coccolithus pelagicus* (s.l., see Figure 4b) peaks (35%) at 19.7 Ma. Increased contributions by *Coccolithus* and small *Reticulofenestra* are observed at ~18 Ma and ~17.5 Ma, respectively.

[24] In addition to their total abundance, contributions of small coccoliths within each genus/morphotype depict important fluctuations in algal physiology and productivity, especially within the reticulofenestrids (Figures 4d and 4e). Notably, fossilized reticulofenestrid coccospheres were smallest and most abundant in the sample dating ~20.3 Ma, coinciding with strong surface water stratification inferred from foraminiferal $\delta^{18}O$ values and maximum $\varepsilon_{p37:2}$ estimates [*Pagani et al.*, 2000].

5.2. Reticulofenestrid Cell Geometry

[25] A total of 55 intact fossil reticulofenestrid coccospheres were identified in a suite of samples of early Miocene, Oligocene and Eocene age (auxiliary material Table S2), providing the opportunity to quantify the relationship between coccosphere, algal cell and coccolith dimensions. Mean cell and coccosphere diameter for these specimens are linearly correlated (Figure 5a; r^2 = 0.93, p value < 0.0001). Similarly, mean coccolithophore cell diameter (D_{cell}) is linearly correlated to coccolith length ($L_{coccolith}$) (Figure 5b; r^2 = 0.82, p value < 0.0001). Therefore ancient cell sizes of alkenone producers can be estimated by

$$D_{cell} = 0.55 + 0.88 L_{coccolith} \quad (7)$$

with coccolith length and cell diameter in μm. Cell volume and surface area were subsequently calculated assuming simple spherical geometry.

[26] Changes in mean haptophyte cell size during the early Miocene are scaled to cell dimensions of modern *E. huxleyi* in nitrate-limited chemostat cultures, with cell radius = 2.6 ± 0.3 μm [*Bidigare et al.*, 1997; *Popp et al.*, 1998]. At similar coccolith dimensions [*Young and Westbroek*, 1991], modern *E. huxleyi* appears to have ~50% larger cell diameters than its Miocene ancestors (Figure 5b). However, coccosphere dimensions (including coccoliths) of modern *E. huxleyi* appear to fit the Miocene relationship between fossil reticulofenestrid coccosphere diameter versus coccolith size (Figure 6). This suggests that *E. huxleyi* produces more thinly calcified coccoliths (coccolith thickness ~0.5 μm) relative to Miocene haptophytes (coccolith thickness >1 μm). Alternatively, the number of coccoliths surrounding each cell has increased in modern *E. huxleyi*, which reportedly can be up to 23 [*Knappertsbusch*, 1993], compared to 10–12 in the fossil reticulofenestrid coccospheres observed in this study.

5.3. Reticulofenestrid Coccolith Size Variation

[27] Before 21 Ma, mean reticulofenestrid coccolith sizes were ~4 μm, comparable to modern *E. huxleyi* Type B coccoliths [*Young and Westbroek*, 1991] (Figure 5b), with an increased total range in sizes at ~21.5 Ma and during the latest Oligocene (Figure 7 and auxiliary material Table S3). The smallest mean reticulofenestrid coccolith sizes (~3.5 μm) comparable to modern *E. huxleyi* Type A coccoliths [*Young and Westbroek*, 1991], are found between ~21 to 20 Ma prior to a marked increase to mean sizes of 5 to 6.5 μm from 19.7 Ma onward. The same trend is most pronounced in the 95th percentile sizes (the measured size value separating the largest 5% of the reticulofenestrid assemblage from the smaller 95%) whereas the lower size limit (5th percentile sizes) remains relatively stable. This points to strong diversification within the reticulofenestrids after 20 Ma, incorporating ever larger (morpho-) species in the phytoplankton community.

[28] Mean coccolithophore cell diameter and $V:SA_{fossil}$ were estimated using the mean coccolith size (± 95% confidence interval of the mean) and equation (7). As discussed above (Section 4.2), cell diameters estimated for early Miocene reticulofenestrids are smaller relative to modern *E. huxleyi* in chemostat culture at comparable coccolith sizes (Figure 5b). In general, mean $V:SA_{fossil}$ estimates are inversely proportional to $\varepsilon_{p37:2}$ values (Figure 8), with significantly smaller cell dimensions corresponding to higher $\varepsilon_{p37:2}$ estimates before 20.3 Ma and between 18–17 Ma.

6. Discussion

[29] Our results demonstrate that substantial changes in cell geometry and nannofossil assemblages occurred in concert with changes in $\varepsilon_{p37:2}$. Measured $\varepsilon_{p37:2}$ and inferred V:SA values are anticorrelated (Figures 8a and 8b) and strongly suggest that larger cell sizes have, in part, influenced the large ~6‰ decrease in $\varepsilon_{p37:2}$ after

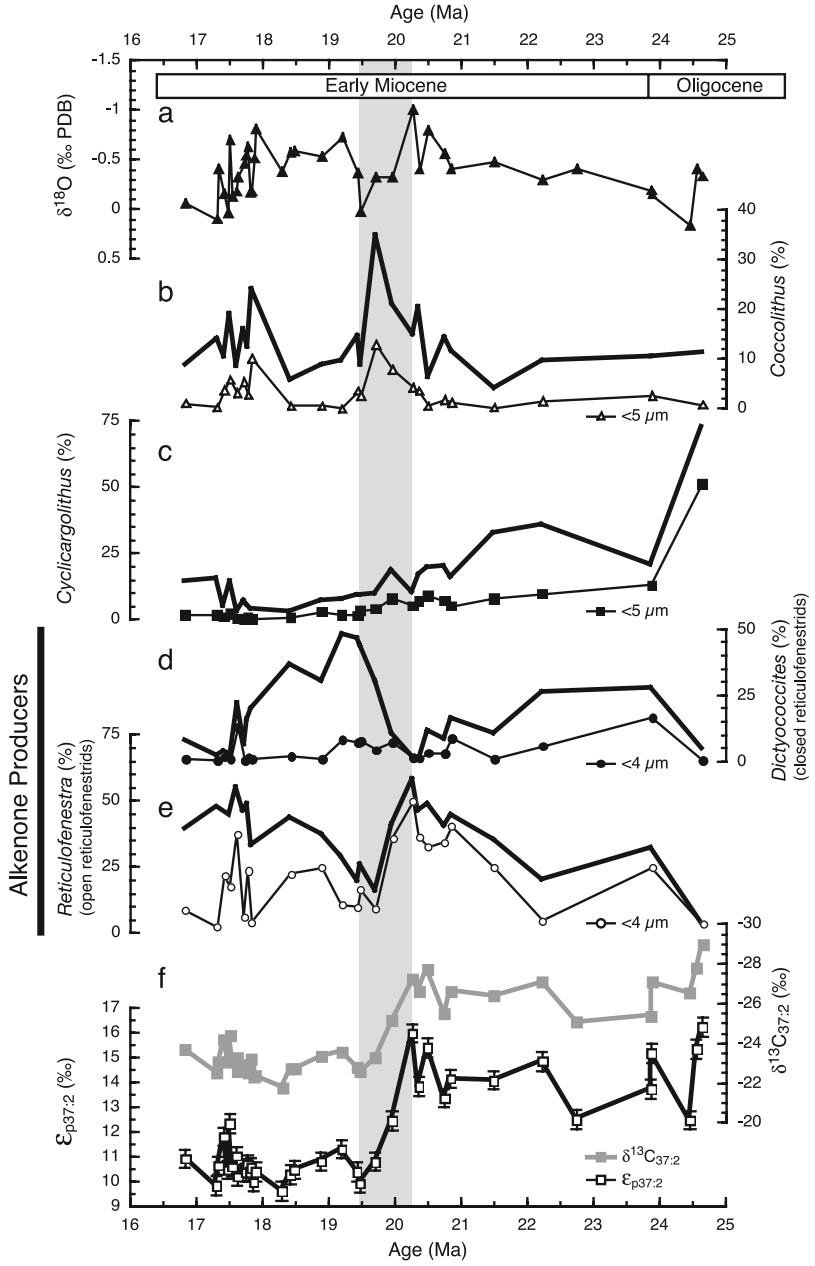

Figure 4. Selected geochemical proxy data (Figures 4a and 4f) and nannofossil assemblage data (Figures 4b–4e) at Site 516. (a) Stable oxygen isotopic composition of shallow dwelling planktonic foraminifera [*Pagani et al.*, 2000]; cumulative relative abundances of major genera, including patterns of selected small morphotypes/species: (b) *Coccolithus*, (c) *Cyclicargolithus*, (d) *Dictyococcites* (equal to heavily calcified *Reticulofenestra*), and (e) *Reticulofenestra*; and (f) stable carbon isotopic composition of alkenones ($\delta^{13}C_{alk}$, grey symbols) and alkenone-derived $\varepsilon_{p37:2}$ record (open symbols) [*Pagani et al.*, 2000]. The grey area indicates the large ~6‰ decrease in $\varepsilon_{p37:2}$ between ~20.3 and ~19.5 Ma.

~20.3 Ma. Such changes have important implications on the interpretation of algal growth rate and/or pCO_2 inferred from $\varepsilon_{p37:2}$ values. For example, if relatively constant surface water concentrations of $CO_{2(aq)}$ (e.g., 6–10 μmol kg^{-1} [see *Pagani et al.*, 2000]) are assumed, then changes in growth rates can be evaluated by considering the effect of cell geometry on the term $K_{V:SA}$ (equations (4) and (5b) and Figure 8c). Opposite trends in cell size and mean growth rates is expected from our mathematical premise as well as biology given that smaller coccolithophores have significantly faster growth rates than larger ones in culture [e.g., *Ziveri et al.*, 2003]. Reconstructed growth rates increase from ~21 to 20 Ma, followed by a more steady decline to ~18.5 Ma. Importantly, the net change in haptophyte growth rates between 20.3 and 19.5 Ma amounts to a ~16% increase.

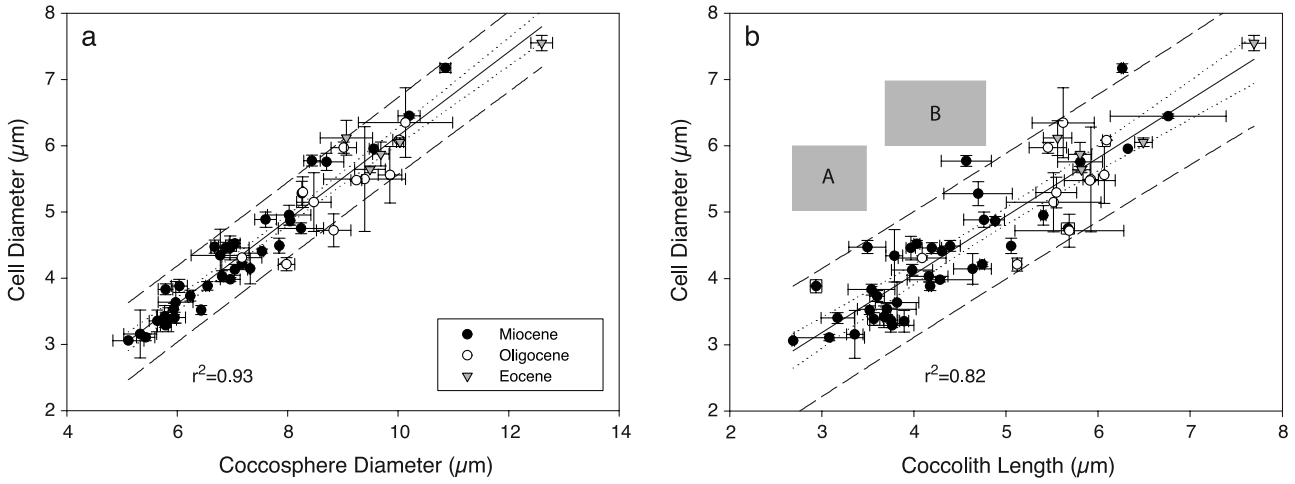

Figure 5. Empirical linear relationships between reticulofenestrid (a) coccosphere and cell diameter ($y = -0.20 + 0.63x$ with $r^2 = 0.93$, p value < 0.0001) and (b) cell diameter and coccolith length ($y = 0.55 + 0.88x$, with $r^2 = 0.82$, p value < 0.0001). $N = 55$. Error bars represent minimum and maximum estimates. Note different symbols for coccospheres encountered in Miocene, Oligocene, and Eocene samples. The least squares linear regression derived in Figure 5b was used to reconstruct cell geometries from measured mean coccolith sizes (shown in Figure 7). The 95% confidence intervals (dotted) and 95% prediction bands (dashed) of regressions are indicated. Grey boxes in (Figure 5b) depict modern *E. huxleyi* cell and coccolith dimensions for genotypes A and B [*Young and Westbroek*, 1991].

[30] If constant, low nutrient concentrations are assumed, then an evaluation of $CO_{2(aq)}$ is possible. Assuming a range of $[PO_4]$ between 0.2–0.4 μM, the physiologically dependent term "*b*" can be corrected using changes in V:SA, relative to modern *E. huxleyi* cell dimensions (equations (4), (6b), and (7)). This exercise results in lower estimates of $CO_{2(aq)}$ that fluctuate between 6–11 μmol kg^{-1} (grey band in Figure 8d). Consequently, our revised atmospheric pCO_2 calculations result in overall low values during the early Miocene (<350 ppmv; Figure 9). These revised $CO_{2(aq)}$ and pCO_2 estimates are now more similar to other alkenone-based Miocene reconstructions from oligotrophic Sites 588 (southwest Pacific) and 608 (North Atlantic) [*Pagani et al.*, 1999].

[31] Arguably, our record of reticulofenestrid V:SA could be interpreted as a qualitative measure of changes in $CO_{2(aq)}$. One mechanistic explanation for changes in cell size is that the carbon cell^{-1}-to-surface area ratio (or V:SA) controls the net flux of CO_2 [e.g., *Laws et al.*, 1995]. In light of cellular carbon demand for photosynthesis, haptophyte cells may therefore vary their cell size in response to variable $CO_{2(aq)}$. In this model, the dominance of small reticulofenestrids prior to 20 Ma would represent a period of low $CO_{2(aq)}$, potentially limiting the photosynthetic capacity of larger cells, while the gradual addition of larger morphospecies that followed would be consistent with a response to elevated ambient $CO_{2(aq)}$. However, evaluation of our data (Figures 8 and 9) and published modern species-specific responses to variable $CO_{2(aq)}$ does not support this hypothesis for the early Miocene. In culture experiments, both small (*E. huxleyi* and *G. oceanica*) and large (*C. leptoporus* and *C. pelagicus*) coccolithophores show only minor variability in organic carbon production under large ranges in $CO_{2(aq)}$ [*Riebesell et al.*, 2000; *Zondervan et al.*, 2001; *Langer et al.*, 2006]. In the case of *E. huxleyi* (compare data of *Riebesell et al.* [2000]), a significant decrease in cellular-carbon content (and thus cell volume) was only found under extremely biolimiting, and unnaturally low $CO_{2(aq)}$ (1.1 and 2.7 μmol kg^{-1}; at 16°C, this corresponds to pCO_2 < 100 ppmv). In contrast, experiments under $CO_{2(aq)} \geq$ 4.0 μmol kg^{-1} (and up to 53.5 μmol kg^{-1}) rendered cells with only minor variability in carbon quota (10.2 ± 0.9 (s.d.)

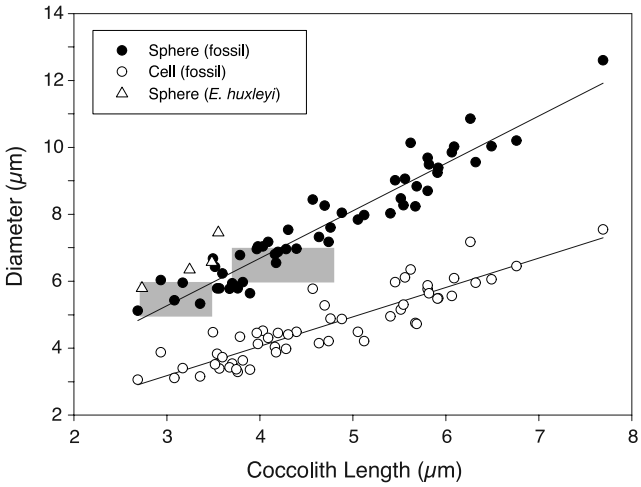

Figure 6. Combined plot of reticulofenestrid coccosphere (solid symbols) and cell diameter (open symbols) versus coccolith length, depicting increasing coccolith thickness with increasing size. Grey boxes are as in Figure 5b. Coccosphere diameters of modern *E. huxleyi* (triangles) closely follow the fossil coccosphere-coccolith size relationship ($y = 1.02 + 1.42x$, $r^2 = 0.92$, p value < 0.0001), but cell diameters are ~50% larger than Miocene reticulofenestrids.

Figure 7. Temporal variability in coccolith size of probable alkenone producers at Site 516. This summary of reticulofenestrid coccolith length (maximum diameter) measurements shows mean (±95% confidence intervals), median, 5th, and 95th percentile sizes. Grey box indicates range in coccolith sizes of modern *E. huxleyi* [*Young and Westbroek*, 1991].

pg carbon cell^{-1}) and no significant correlation between cell size and $CO_{2(aq)}$. Thus, within modern levels of $CO_{2(aq)}$, intraspecific cell size response to $CO_{2(aq)}$ appears minimal. For the early Miocene, minimum $CO_{2(aq)}$ estimates are well above 4.0 μmol kg^{-1} (Figure 8d), and would therefore not influence haptophyte cell dimensions. Moreover, co-occurring cells of the abundant *Coccolithus pelagicus* (Figure 4b) were at least twice as large as the small reticulofenestrids during this time. This argues against ambient levels of $CO_{2(aq)}$ that would be limiting for photosynthesis in larger haptophytes and, in this case, lends no support to explain the strong diversification of reticulofenestrids after ~20 Ma in terms of $CO_{2(aq)}$ variability. Rather, other factors, such as changes in ocean circulation, water column stratification, sea surface temperature and nutrient availability, likely played more important roles in forcing changes in cell geometry.

7. Implications

[32] Previous interpretations of $\varepsilon_{p37:2}$ at Site 516 inferred a 60% increase in haptophyte growth rates to explain an observed 6‰ decrease in $\varepsilon_{p37:2}$ after ~20.3 Ma [*Pagani et al.*, 2000]. These changes were attributed to major shifts in ocean circulation linked to the development of the ACC and northward propagation of AAIW. Consideration of cell geometry substantially reduces this inferred increase in growth rate to ~16%. Nevertheless, changes in haptophyte growth rates are still consistent with paleoceanographic change, which is supported by major shifts in nannofloral assemblages between 21 and 19 Ma. These assemblage changes appear to primarily depict variable sea surface temperature and surface water stratification.

[33] For example, warmer, more strongly stratified surface waters (based on deep and shallow dwelling foraminiferal δ^{18}O values [cf. *Pagani et al.*, 2000]) are dominated by small, bloom-forming reticulofenestrids (~21–20.3 Ma), whereas cooler and more (perhaps storm-) mixed surface waters are characterized by increased productivity of *Coccolithus* spp., most prominently expressed at 19.7 Ma. Diversification, expressed by the expansion of cell sizes within the reticulofenestrids and steadily increasing contributions of large reticulofenestrids, follows the reestablishment of surface water stratification after ~19.5 Ma. In the modern ocean, extensive natural blooms of *E. huxleyi* are associated with highly stratified water during summer months where the mixed layer depth is less than 30m [*Tyrrell and Taylor*, 1996; *Nanninga and Tyrrell*, 1996]. In contrast, high abundances of *Coccolithus pelagicus* are indicative of moderately turbulent waters, characteristic of upwelling and frontal zones [*Wells and Okada*, 1997; *Cachão and Moita*, 2000], and has been used to define northward shifts of the Polar Front Zone in the Southern Ocean during late Pleistocene glacial periods [*Wells and Okada*, 1997]. Therefore, while the evidence presented in this study reduces estimates of growth rate change between 20 to 19 Ma, it continues to support the interpretation that biological and isotopic variability at oligotrophic Site 516 was linked to paleoceanographic changes that influenced temperature and nutrient characteristics of the upper water column [*Pagani et al.*, 2000].

[34] The present study has an inevitable bias toward reconstructing cell dimensions of only the coccolith-bearing haptophytes, because noncalcifying alkenone producers do not fossilize. Today, noncalcifying Isochrysidales that produce alkenones appear restricted to coastal waters and therefore are not likely to represent an important source of alkenones in deep-sea sediments in the past [*Marlowe et al.*, 1990]. However, the cosmopolitan *Emiliania huxleyi* can also exist as noncalcifying cells (as used by, e.g., *Bidigare et al.* [1997]), showing no significant differences in cell dimensions in chemostat culture (B. N. Popp, personal communication, 2006). Therefore we assume that similar variability in cell sizes of all Isochrysidales can be expected in their evolutionary history.

[35] We also recognize that preferential preservation of coccoliths would affect our interpretations. Indeed, a distinct shift toward larger, more heavily calcified coccoliths

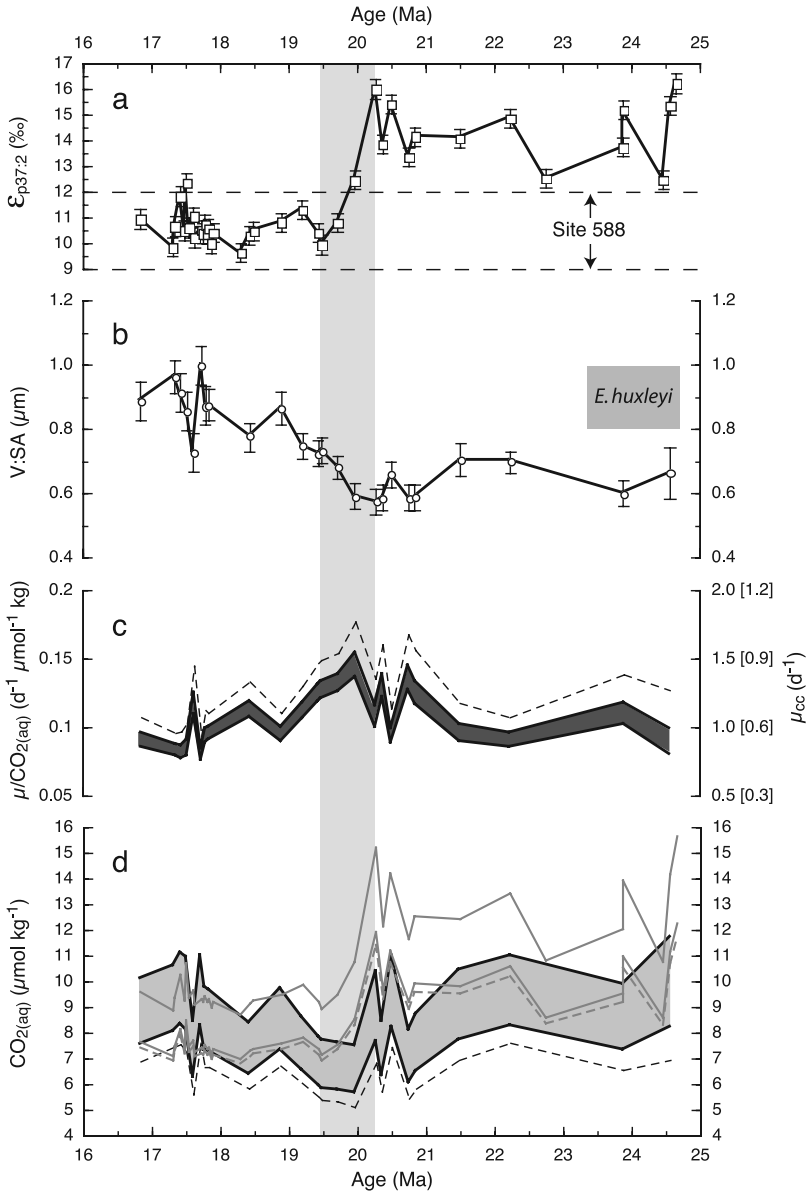

Figure 8. (a) Measured $\varepsilon_{p37:2}$ record at Site 516 [*Pagani et al.*, 2000], with dashed lines indicating the range in $\varepsilon_{p37:2}$ values measured at Site 588 (southwest Pacific [*Pagani et al.*, 1999]). (b) Variability of early Miocene mean $V:SA_{fossil}$, based on mean reticulofenestrid coccolith size (Figure 7) and equation (7). Error bars indicate 95% confidence intervals. Grey box indicates V:SA of modern *E. huxleyi* in chemostat culture [*Popp et al.*, 1998]. (c) Calculated values for $\mu/CO_{2(aq)}$ (left-hand *y* axis) from changes in $K_{V:SA}$ as inferred from (Figure 8b), using equations (4) and (5b). Relative changes in algal growth rates (μ) can be evaluated assuming no changes in ambient CO_2 concentrations. As an example, μ is scaled on the right-hand *y* axis in Figure 8c with constant $CO_{2(aq)} = 10$ μmol kg^{-1} and, in brackets, $CO_{2(aq)} = 6$ μmol kg^{-1}. Grey band depicts minimum and maximum estimates with propagated 95% confidence levels of input factors. Dashed line represents minimum estimates assuming no diagenetic alteration of biogenic carbonates used to determine paleo-SST [see *Pagani et al.*, 2005]. (d) Revised $CO_{2(aq)}$ estimates based on $\varepsilon_{p37:2}$ and cell geometry corrected b', as a function of constant $[PO_4]$ and using equations (2), (6b), and (7), relative to $V:SA_{Ehux} = 0.9(\pm 0.1)$ μm. Grey lines depict $CO_{2(aq)}$ estimates if no cell size corrections were made, following *Pagani et al.* [1999, 2005]. Grey band and dashed line are as in Figure 8c. Minimum values are calculated with lower 95% confidence interval of $V:SA_{fossil}$ and $[PO_4] = 0.2$ μM, maximum with upper 95% confidence interval of $V:SA_{fossil}$ and $[PO_4] = 0.4$ μM. Vertical grey area is as in Figure 4.

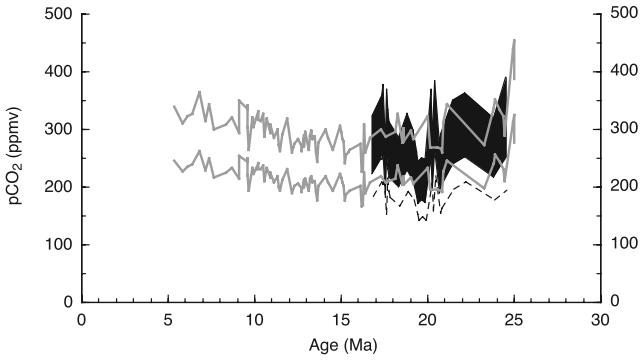

Figure 9. Revised pCO_2 estimates at Site 516 (in black) after haptophyte cell size corrections to $CO_{2(aq)}$ as shown in Figure 8d. New early Miocene pCO_2 values are <350 ppmv, consistent with those reported from other oligotrophic sites (e.g., Site 588, shown in grey [*Pagani et al.*, 1999]).

within a sediment sample could indicate preferential dissolution of smaller, more fragile coccoliths. There are several observations that argue against this conclusion: (1) Coccolith preservation at Site 516 is good, with no or only minor local etching of the distal shields, and consistent throughout the investigated record, and (2) a secular increase in the size of the largest reticulofenestrid coccoliths, while the smallest sizes remain rather constant, cannot be explained by selective dissolution of the small ones. Finally, it would appear rather remarkable that samples containing predominantly small coccoliths correspond consistently to higher $\varepsilon_{p37:2}$ values than samples with larger coccoliths. Therefore we conclude that our observations and morphometric measurements capture primary changes in nannofossil ecology.

8. Conclusions

[36] The relationship between photosynthetic carbon isotope fractionation and $CO_{2(aq)}$ can be affected by a variety of physiological and environmental factors [e.g., *Laws et al.*, 1995, 2001; *Rost et al.*, 2002; *Cassar et al.*, 2006]. Ideally, all factors need to be constrained in order to improve alkenone-based estimates of paleo-pCO_2. In this study, we have taken an important first step to quantify ancient haptophyte cell size variability and its influence on paleo-$\varepsilon_{p37:2}$ records.

[37] With relatively simple measurements of individual coccoliths it is possible to accurately reconstruct cell diameters of extinct species of coccolithophores. Targeting the most probable alkenone producers during the Cenozoic, species belonging to the *Reticulofenestra* and *Dictyococcites* genus (the reticulofenestrids), we show that a marked increase in cell size coincides with a distinct offset in carbon isotopic composition in alkenones. Changes in cell size explain the majority of the observed variability in alkenone-based $\varepsilon_{p37:2}$ values during the early Miocene at DSDP Site 516. Previous interpretations invoked a large 60% increase in haptophyte growth rates to explain a 6‰ decrease in $\varepsilon_{p37:2}$ between 20.3 and 19.5 Ma [*Pagani et al.*, 2000]. Our new data suggest only minor changes in growth rates, not exceeding ~16%. The novel cell size corrections to $CO_{2(aq)}$ estimates also reveal revised values and trends that are more consistent with the global pattern of early Miocene pCO_2 [*Pagani et al.*, 1999].

[38] Until additional deep-sea records are studied, we cannot speculate beyond the local extent of the observed shifts in calcareous phytoplankton community structure and speciation within the reticulofenestrids. The opening of Drake Passage could have played an important role in changing surface current and atmospheric circulation, by causing latitudinal shifts in oceanic fronts toward Site 516 and influencing surface water stratification. However, support for this supposition depends on a better understanding of the timing for the development of the Drake Passage [e.g., *Barker and Thomas*, 2004].

[39] **Acknowledgments.** We would like to thank Brian Popp and one anonymous reviewer for their constructive reviews. This study used Deep Sea Drilling Project samples provided by the Ocean Drilling Program. Research was supported by Swedish Research Council grant VR621-2003-3614 to J.H. and a grant from the National Science Foundation to M.P.

References

Backman, J., and J. O. R. Hermelin (1986), Morphometry of the Eocene nannofossil *Reticulofenestra umbilicus* lineage and its biochronological consequences, *Palaeogeogr. Palaeoclimatol. Palaeoecol.*, *57*, 103–116.

Barker, P. F. (1983), Tectonic evolution and subsidence history of the Rio Grande Rise, *Initial Rep. Deep Sea Drill. Proj.*, *72*, 953–976.

Barker, P. F., and J. Burrell (1977), The opening of the Drake Passage, *Mar. Geol.*, *25*, 15–34.

Barker, P. F., and J. Burrell (1982), The influence upon Southern Ocean circulation, sedimentation, and climate of the opening of Drake Passage, in *Antarctic Geoscience*, edited by C. Craddock, pp. 377–385, Univ. of Wis., Madison.

Barker, P. F., and E. Thomas (2004), Origin, signature and palaeoclimatic influence of the Antarctic circumpolar current, *Earth Sci. Rev.*, *66*, 143–162.

Beaufort, L. (1992), Size variations in late Miocene *Reticulofenestra* and implication for paleoclimatic interpretation, *Mem. Sci. Geol.*, *43*, 339–350.

Belkin, I. M., and A. L. Gordon (1996), Southern Ocean fronts from the Greenwich meridian to Tasmania, *J. Geophys. Res.*, *101*, 3675–3696.

Bidigare, R. R., et al. (1997), Consistent fractionation of ^{13}C in nature and in the laboratory: Growth-rate effects in some haptophyte algae, *Global Biogeochem. Cycles*, *11*, 279–292, (Correction, *Global Biogeochem. Cycles, 13*, 251–252, 1999.)

Bollmann, J., B. Brabec, M. Y. Cortes, and M. Geisen (1999), Determination of absolute coccolith abundances in deep-sea sediments by spiking with microbeads and spraying (SMS-method), *Mar. Micropaleontol.*, *38*, 29–38.

Burkhardt, S., U. Riebesell, and I. Zondervan (1999), Effects of growth rate, CO_2 concentration, and cell size on the stable carbon isotope fractionation in marine phytoplankton, *Geochim. Cosmochim. Acta*, *63*, 3729–3741.

Cachão, M., and T. Moita (2000), *Coccolithus pelagicus*, a productivity proxy related to moderate fronts off western Iberia, *Mar. Micropaleontol.*, *39*, 131–155.

Cassar, N., E. A. Laws, and B. N. Popp (2006), Carbon isotopic fractionation by the marine diatom *Phaeodactylum tricornutum* under nutrient- and light-limited growth conditions, *Geochim. Cosmochim. Acta*, *70*, 5323–5335.

Conte, M., A. Thompson, G. Eglinton, and J. C. Green (1995), Lipid biomarker diversity in the coccolithophorid *Emiliania huxleyi* (Prymnesiophyceae) and the related species *Gephyrocapsa oceanica*, *J. Phycol.*, *31*, 272–282.

Freeman, K. H., and J. M. Hayes (1992), Fractionation of carbon isotopes by phytoplankton and estimates of ancient CO_2 levels, *Global Biogeochem. Cycles*, *6*, 185–198.

Fujiwara, S., M. Tsuzuki, M. Kawachi, N. Minaka, and I. Inouye (2001), Molecular phylogeny of the Haptophyta based on the rbcL gene and sequence variation in the spacer region of the Rubisco operon, *J. Phycol.*, *37*, 121–129.

Henderiks, J., and A. Törner (2006), Reproducibility of coccolith morphometry: Evaluation of spraying and smear slide preparation techniques, *Mar. Micropaleontol.*, *58*, 207–218.

Jasper, J. P., and J. M. Hayes (1990), A carbon isotope record of CO_2 levels during the late Quaternary, *Nature*, *347*, 462–464.

Jasper, J. P., J. M. Hayes, A. C. Mix, and F. G. Prahl (1994), Photosynthetic fractionation of ^{13}C and concentrations of dissolved CO_2 in the central equatorial Pacific during the last 255000 years, *Paleoceanography*, *9*, 781–798.

Johnson, T. C. (1983), Regional oceanographic setting of the southwestern Atlantic, *Initial Rep. Deep Sea Drill. Proj.*, *72*, 15–35.

Kameo, K., and T. Takayama (1999), Biostratigraphic significance of sequential size variations of the calcareous nannofossil genus *Reticulofenestra* in the upper Pliocene of the North Atlantic, *Mar. Micropaleontol.*, *37*, 41–52.

Knappertsbusch, M. (1993), Geographic distribution of living and Holocene coccolithophores in the Mediterranean Sea, *Mar. Micropaleontol.*, *21*, 219–247.

Langer, G., M. Geisen, K.-H. Baumann, J. Kläs, U. Riebesell, S. Thoms, and J. R. Young (2006), Species-specific responses of calcifying algae to changing seawater carbonate chemistry, *Geochem. Geophys. Geosyst.*, *7*, Q09006, doi:10.1029/2005GC001227.

Laws, E. A., B. N. Popp, R. R. Bidigare, M. C. Kennicutt, and S. A. Macko (1995), Dependence of phytoplankton carbon isotopic composition on growth rate and $[CO_2]_{aq}$: Theoretical considerations and experimental results, *Geochim. Cosmochim. Acta*, *59*, 1131–1138.

Laws, E. A., B. N. Popp, R. R. Bidigare, U. Riebesell, S. Burkhardt, and S. G. Wakeham (2001), Controls on the molecular distribution and carbon isotopic composition of alkenones in certain haptophyte algae, *Geochem. Geophys. Geosyst.*, *2*(1), doi:10.1029/2000GC000057.

Marlowe, I. T., S. C. Brassell, G. Eglinton, and J. C. Green (1990), Long-chain alkenones and alkyl alkenoates and the fossil coccolith record of marine sediments, *Chem. Geol.*, *88*, 349–375.

McIntyre, T. C., A. W. H. Bé, and R. Prekistas (1967), Coccoliths and the Pliocene-Pleistocene boundary, in *Progress in Oceanography*, edited by M. Sears, pp. 3–25, Pergamon, New York.

Montagnes, D. J. S., J. A. Berges, P. J. Harrison, and F. J. R. Taylor (1994), Estimating carbon, nitrogen, protein, and chlorophyll a from volume in marine phytoplankton, *Limnol. Oceanogr.*, *39*, 1044–1060.

Nanninga, H. J., and T. Tyrrell (1996), The importance of light for the formation of algal blooms by *Emiliania huxleyi*, *Mar. Ecol. Progr. Ser.*, *136*, 195–203.

Pagani, M., M. A. Arthur, and K. H. Freeman (1999), Miocene evolution of atmospheric carbon dioxide, *Paleoceanography*, *14*, 273–292.

Pagani, M., M. A. Arthur, and K. H. Freeman (2000), Variations in Miocene phytoplankton growth rates in the southwest Atlantic: Evidence for changes in ocean circulation, *Paleoceanography*, *15*, 486–496.

Pagani, M., J. C. Zachos, K. H. Freeman, B. Tripple, and S. Bohaty (2005), Marked decline in atmospheric carbon dioxide concentrations during the Paleogene, *Science*, *309*, 600–603.

Pearson, P. N., and M. R. Palmer (2000), Atmospheric carbon dioxide concentrations over the past 60 million years, *Nature*, *406*, 695–699.

Peterson, R. G., and T. Whitworth III (1989), The subantarctic and polar fronts in relation to deep water masses through the southwestern Atlantic, *J. Geophys. Res.*, *94*, 10,817–10,838.

Popp, B. N., E. A. Laws, R. R. Bidigare, J. E. Dore, K. L. Hanson, and S. G. Wakeham (1998), Effect of phytoplankton cell geometry on carbon isotopic fractionation, *Geochim. Cosmochim. Acta*, *62*, 69–77.

Raffi, I., J. Backman, E. Fornaciari, H. Pälike, D. Rio, L. Lourens, and F. Hilgen (2006), A review of calcareous nannofossil astrobiochronology encompassing the past 25 million years, *Quat. Sci. Rev.*, *25*, 3113–3137.

Rau, G. H., T. Takahashi, and D. J. Des Marais (1989), Latitudinal variations in plankton $\delta^{13}C$: Implications for CO_2 and productivity in past oceans, *Nature*, *341*, 516–518.

Rau, G. H., T. Takahashi, D. J. Des Marais, D. J. Repeta, and J. H. Martin (1992), The relationship between delta^{13}C of organic matter and CO_2(aq) in ocean surface water: Data from a JGOFS site in the northeast Atlantic Ocean and a model, *Geochim. Cosmochim. Acta*, *56*, 1413–1419.

Riebesell, U., A. Revill, D. G. Holdsworth, and J. K. Volkman (2000), The effects of varying CO_2 concentration on lipid composition and carbon isotope fractionation in Emiliania huxleyi, *Geochim. Cosmochim. Acta*, *64*, 4179–4192.

Rosell-Melé, A., P. Comes, P. J. Müller, and P. Ziveri (2000), Alkenone fluxes and anomalous UK′37 values during 1989–1990 in the northeast Atlantic (48°N 21°W), *Mar. Chem.*, *71*, 251–264.

Rost, B., I. Zondervan, and U. Riebesell (2002), Light-dependent carbon isotope fractionation in the coccolithophorid *Emiliania huxleyi*, *Limnol. Oceanogr.*, *47*, 120–128.

Royer, D. L., R. A. Berner, and D. J. Beerling (2001), Phanerozoic atmospheric CO_2 change: Evaluating geochemical and paleobiological approaches, *Earth Sci. Rev.*, *54*, 349–392.

Sáez, A. G., I. Probert, M. Geisen, P. Quinn, J. Young, and L. K. Medlin (2003), Pseudocryptic speciation in coccolithophores, *Proc. Natl. Acad. Sci. U. S. A.*, *100*, 7163–7168.

Scher, H. D., and E. E. Martin (2004), Circulation in the Southern Ocean during the Paleogene inferred from neodymium isotopes, *Earth Planet. Sci. Lett.*, *228*, 391–405.

Siegenthaler, U., et al. (2005), Stable carbon cycle-climate relationship during the late Pleistocene, *Science*, *310*, 1313–1317.

Thierstein, H. R., K. R. Geitzenauer, B. Molfino, and N. J. Shackleton (1977), Global synchroneity of late Quaternary coccolith datum levels: Validation by oxygen isotopes, *Geology*, *5*, 400–404.

Tyrrell, T., and A. H. Taylor (1996), A modelling study of *Emiliania huxleyi* in the NE Atlantic, *J. Mar. Syst.*, *9*, 83–112.

Van der Burg, J., H. Visscher, D. L. Dilcher, and W. M. Kürschner (1993), Paleoatmospheric signatures in Neogene fossil leaves, *Science*, *260*, 1788–1790.

Verity, P. G., C. Y. Robertson, C. R. Tronzo, M. G. Andrews, J. R. Nelson, and M. E. Sieracki (1992), Relationships between cell volume and the carbon and nitrogen content of marine photosynthetic nanoplankton, *Limnol. Oceanogr.*, *37*, 1434–1446.

Volkman, J. K. (2000), Ecological and environmental factors affecting alkenone distributions in seawater and sediments, *Geochem. Geophys. Geosyst.*, *1*(9), doi:10.1029/2000GC000061.

Volkman, J. K., S. Barrett, S. Blackburn, and E. Sikes (1995), Alkenones in *Gephyrocapsa oceanica*: Implications for studies of paleoclimate, *Geochim. Cosmochim. Acta*, *59*, 513–520.

Wells, P., and H. Okada (1997), Response of nannoplankton to major changes in sea-surface temperature and movements of hydrological fronts over Site DSDP 594 (south Chatham Rise, southeastern New Zealand), during the last 130 kyr, *Mar. Micropaleontol.*, *32*, 341–363.

Westbroek, P. C., et al. (1993), A model system approach to biological climate forcing: The example of *Emiliania huxleyi*, *Global Planet. Change*, *8*, 27–46.

Wise, S. W. J. (1983), Mesozoic and Cenozoic calcareous nannofossils recovered by Deep Sea Drilling Project Leg 71 in the Falkland Plateau region, southwest Atlantic Ocean, *Initial Rep. Deep Sea Drill. Proj.*, *71*, 481–550.

Young, J. (1990), Size variation of Neogene *Reticulofenestra* coccoliths from Indian Ocean DSDP cores, *J. Micropaleontol.*, *9*, 71–86.

Young, J. (1998), Neogene, in *Calcareous Nannofossil Biostratigraphy*, edited by P. Bown, pp. 225–265, Chapman and Hall, Cambridge, U. K.

Young, J., and P. Westbroek (1991), Genotypic variation in the coccolithophorid species *Emiliania huxleyi*, *Mar. Micropaleontol.*, *18*, 5–23.

Young, J. R., J. M. Didymus, P. R. Bown, B. Prins, and S. Mann (1992), Crystal assembly and phylogenetic evolution in heterococcoliths, *Nature*, *356*, 516–518.

Ziveri, P., H. M. Stoll, I. Probert, C. Klaas, M. Geisen, G. Ganssen, and J. Young (2003), Stable isotope 'vital effects' in coccolith calcite, *Earth Planet. Sci. Lett.*, *210*, 137–149.

Zondervan, I., R. E. Zeebe, B. Rost, and U. Riebesell (2001), Decreasing marine biogenic calcification: A negative feedback on rising atmospheric pCO_2, *Global Biogeochem. Cycles*, *15*, 507–516.

J. Henderiks, Department of Geology and Geochemistry, Stockholm University, SE-106 91, Stockholm, Sweden. (jorijntje.henderiks@geo.su.se)

M. Pagani, Department of Geology and Geophysics, Yale University, P.O. Box 208109, New Haven, CT 06520, USA.